A Novel High-Performance Mission-Enabling Multi-Purpose Radioisotope Heat Source

Michael J. Durka
Jet Propulsion Laboratory
California Institute of Technology
Pasadena, CA, USA
michael.j.durka@jpl.nasa.gov

Jean-Pierre Fleurial
Jet Propulsion Laboratory
California Institute of Technology
Pasadena, CA, USA
jean-pierre.fleurial@jpl.nasa.gov

Sarah E. Wielgosz
Mechanical Engineering
University of Pittsburgh
Pittsburgh, PA, USA
saw179@pitt.edu

Shane P. Riley
Mechanical Engineering
University of Pittsburgh
Pittsburgh, PA, USA
shane.riley@pitt.edu

Matthew M. Barry
Mechanical Engineering
University of Pittsburgh
Pittsburgh, PA, USA
matthew.michael.barry@pitt.edu

David F. Woerner
Jet Propulsion Laboratory
California Institute of Technology
Pasadena, CA, USA
david.f.woerner@jpl.nasa.gov

Brian Barstow
Jet Propulsion Laboratory
California Institute of Technology
Pasadena, CA, USA
brian.barstow@jpl.nasa.gov

Fivos Drymiotis
Jet Propulsion Laboratory
California Institute of Technology
Pasadena, CA, USA
fivos.drymiotis@jpl.nasa.gov

Bill J. Nesmith
Jet Propulsion Laboratory
California Institute of Technology
Pasadena, CA, USA
bill.j.nesmith@jpl.nasa.gov

***Abstract*—Recent studies indicate science mission concepts targeting access to the sub-surface oceans of icy moons require ice-penetrating cryobots powered by advanced Radioisotope Power Systems (RPS). These systems would deliver waste heat for ice-melting in the range of 10 kW. Minimizing the transit time through the kilometers-thick ice shells to just a few years requires these RPS to utilize heat sources having a higher thermal energy volumetric density than the existing flight-qualified General-Purpose Heat Source (GPHS). A Compact Heat Source (CPHS) has been conceptualized in which the graphite impact shells (GIS) of the existing GPHS would be rearranged in a hexagonal aeroshell containing seven GIS per module, as opposed to the standard two per module; offering a thermal energy density of 0.57 W/cm^3 versus 0.29 W/cm^3 offered by the GPHS simply from the repackaging of Technology Readiness Level (TRL) 9 subassemblies. Preliminary thermal modeling of the CPHS integrated into a notional radioisotope thermoelectric generator (RTG) structure further suggests that centerline temperatures are well within allowable limits during nominal operation.**

Given the need for the CPHS for a subset of mission concepts, it is worth exploring the applicability of the CPHS for more general RTG purposes. We discuss herein how the CPHS may be implemented with either heritage or in-development thermoelectric converter technologies into a Next-Generation RTG concept. Due to a higher energy density, the legacy heat rejection fin arrangement must be modified to permit a sufficiently low cold-side temperature. Preliminary finite element analysis suggests fin-root temperatures could be kept as low as 520 K while allowing the generator to fit within the usable dimensions of currently available United States Department of Energy shipping containers. Such temperatures would certainly be compatible with the use of high temperature thermoelectric converter technologies.

A prime candidate is the heritage silicon-germanium (SiGe) unicouple, whose design could be adapted by approximately halving the leg-length, but without changes in hot and cold junction interfaces, which are features critical to the proven performance and reliability of these devices. The estimated Beginning of Life power for a SiGe-based CPHS-RTG using 12 CPHS for a thermal inventory of 10.5 kW is greater than 600 W under deep space operating conditions. Using higher performance segmented couples currently in development that are based on skutterudite, $La_{3-x}Te_4$ and 14-1-11 Zintl thermoelectric materials in lieu of the SiGe unicouples would increase the power level to more than 1 kW.

The high specific power (W_e/kg) attribute of CPHS-RTGs found in this study could potentially enable Radioisotope Electric Propulsion (REP) mission concepts. Past NASA REP mission concept studies identified specific power needs in excess of 6 to 8 W_e/kg. Based on a GPHS-RTG-like system configuration, we show that at fin root temperatures between 530 K and 570 K (deep space environment), specific powers exceeding 10 W_e/kg are achievable using high performance segmented thermoelectric converters. The compact sizing and power density of the CPHS-RTG would constitute a significant step upgrade in specific power when compared to heritage GPHS-RTG (approximately 5.1 W_e/kg) and off-the-shelf Multi-Mission RTG (approximately 2.6 W_e/kg).

***Index Terms*—Radioisotope thermoelectric generator, Deep space power generation, Compact heat source**

I. Introduction

The search for extra-terrestrial life in our solar system is one of the foremost goals in planetary exploration. The Outer Planets Assessment Group (OPAG) have proposed sub-surface ocean access life-detection missions to Europa and

Enceledus [1]. The completion of the Europa Clipper flagship mission will enhance current knowledge of the Europan ice shelf, providing necessary information for a sub-surface access mission, making Europa a prime target for a life detection mission. Such a mission requires an ice probe, or cryobot, to melt through tens of kilometers of ice to access the sub-surface ocean.

Cryobots have been successfully deployed in terrestrial applications over five decades. In such an application, gravity forces the probe to rest on a thin water film beneath which ice is warmed and melted. The probe descends, forcing the effluent water upwards (against gravity) through a water annulus surrounding the probe. Sufficient heat to maintain this channel through which to displace effluent water must be supplied. The thermal requirements for such a terrestrial-based system have been previously characterized [5], and the required annulus thickness for extraterrestrial-focused systems has been quantified [4].

The operation of a cryobot in a similar manner on Europa however changes many requirements from terrestrial iceprobes. The required distance to traverse is orders of magnitude higher [3], and the power source must be self contained. It has been previously assessed that radioisotope power systems (RPS) are the only known viable technologically available means of powering such a mission for the foreseeable future [2]. The aforementioned study furthermore assesses that the form factor of the currently flight-qualified heat sources provides an insufficient thermal power density for mission completion in a practical duration and with a feasible system mass. As a result, Woerner et al. [2] recommended the repackaging of two graphite impact shells (GIS) contained within the brick-shaped flight-qualified general purpose heat source (GPHS) into a more-circular 7-GIS arrangement compact heat source (CPHS) (see Fig. 1. Each CPHS would produce 875 W_t as opposed to the 250 W_t GPHS, and thus would offer a nearly two-fold increase in thermal energy density over the GPHS which would substantially reduce the mission completion time and payload mass (see Fig. 8 in [2]).

While [2] establishes a specific need for a new heat source based on the thermal requirements for cryobot operation on Europa, the study did not address the overall feasibility of such an investment in resources from the perspective of electrical power generation. The successful production of a new heat source, while enabling of cryobot missions, does not alone guarantee the overcoming of other technological and financial challenges inherent to the successful completion of a cryobot mission. One such readily realizable challenge is simply the fulfillment of the proposed energy budget for a Europa ocean-access mission - which currently amounts to roughly 10 kW [2]. Current ^{238}Pu production by the United States Department of Energy (US DOE) is not expected to exceed 1.5 kg per year under current planning. A 10 kW mission would amount to requiring 25 kg of ^{238}Pu; demanding one and a half decades worth of production for a single mission at current rates. Furthermore, the US DOE 9904 shipping container currently

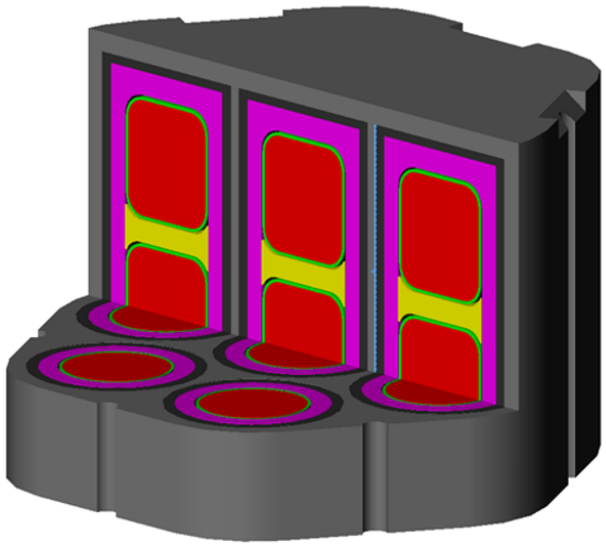

Fig. 1. The notional 7-GIS compact heat source (CPHS). Image taken from [2]. From inside outward, red indicates the ^{238}Pu pellets, green the iridium cladding, yellow the floating membrane, pink the graphite impact shell, black the carbon bonded carbon fiber sleeve, and finally, grey is the aeroshell.

in use was designed[1] to accommodate a 4.5 kW thermal inventory [6]. Shipping and assembly logistics would either need to be modified for the assembly of a cryobot mission to Europa, or procedures to complete the final assembly of the RTG on the premise of the launch site could be an alternative to this modification. As much is required with the development and implementation of a new heat source, it is useful to demonstrate that the CPHS has value as the power source of a RTG for a broader class of missions rather than as exclusively providing compact thermal energy in a cryobot to melt ice.

This work evaluated the potential of the CPHS to serve as the radioisotope thermoelectric generator (RTG) heat source in a cold-space vacuum environment utilizing existing GPHS-based hardware. A high-level, parametric approach is utilized leveraging novel fast-computing codes that assess permutations of the system-level designs at beginning-of-life conditions. Leveraging high-performance computing, the optimal device configurations for RTG power and specific power have been obtained. Specific-power estimates of both the CPHS and GPHS in RTGs are provided utilizing both flight-qualified Silicon Germanium converter materials as well as skutterudite, $La_{3-x}Te_4$ and 14-1-11 Zintl thermoelectric materials pertaining to Next-Generation power conversion systems, denoted as MOD2 converters. In terms of specific power, particular attention is directed towards evaluating a GPHS-like system powered by CPHS heat source(s) to fulfill power requirements for radioelectric propulsion (REP) based missions. To fully assess and compare differences in GPHS versus CPHS based RTG systems, four scenarios are considered in which the maximum specific power is calculated:

[1]The authors refer to the assumed thermal inventory in § 3.5 Hypothetical Thermal Accident Evaluation of [6]

1) GPHS-based RTG varying thermoelectric converter design with existing packaging
2) GPHS-based RTG free-form design allowing geometry of the packaging to change
3) CPHS-based RTG heat source varying thermoelectric converter design with existing packaging
4) CPHS-based RTG heat source free-form design allowing geometry of the packaging to change

Lastly, assessments are made for outlining the practical steps for further in-depth analysis of adapting current RPS systems to utilize the higher CPHS power density more effectively to best establish the CPHS as an alternative general purpose heat source rather than hardware for limited use.

II. Methodology

In the following sections, the design methodology is presented. For brevity, the analytic modeling is discussed, but the reader is referred to the consulted works from greater detail.

A. Design Parameters

Finding the optimal specific power for a RTG containing a novel heat source requires consideration of many design parameters (i.e., converter length, segment temperatures, cold junction temperatures, to name some) that interact with each-other. To make such an analysis tractable, a multi-variable parametric approach was taken. In this trade study, the parameters considered are listed in Table I. Design constraints considered in all analyses are listed in Table II.

B. Procedural Overview

The calculation of specific power for a CPHS RTG is comprised of two analyses: the rejection of thermal waste-heat to space and the thermoelectric generation of electrical power. Both analyses are intrinsically coupled, as the temperature at which the radiator rejects the thermal load to space determines the thermometric performance of the generator. The RTG was presumed housed in a cylindrical Al2219 housing having a 22.25 cm outer diameter with 2.25 mm thickness - similar to current multi-mission RTG (MMRTG) dimensions. Trade studies with eight and 16 circular Al6063 fins of varying length were conducted to determine the fin root temperature as a function of the sum of fin and housing mass. The axial length was taken as two heat-source axial length, and the system thermal inventory, length, and heat source mass was taken as linear with the number of heat sources used. The impact of different device lengths on the fins' radiation view factor is currently neglected for the present high-level analysis. As such, the difference between the cold junction temperature and the fin root temperature is assumed to be constant.

The remainder of the system mass excluding the thermal-electric converter material was approximated based on existing mass per unit length data from [7] with the housing end cap masses independent of generator length, and the heat source masses were derived from the mass of the GPHS-Step2 module [9] . The thermometric cold-junction temperatures finally were assumed to be 20 and 30 K greater than the fin root temperatures for GPHS and CPHS-based RTGs respectively, thus allowing the system mass (excluding the thermoelectric converter legs) to be related to the cold junction temperature. With this relationship known, it was then possible to compute the thermoelectric power per unit system mass.

For each thermoelectric computation per system-level mass and thermal inventory, a hot-junction temperature limitation of 1273 K was imposed. Each converter design permutation was designed to comprise of four parallel strings having a 30 V potential. The low temperature segment length and area for each leg, as well as cold junction temperature and load resistance, were all allowed to float along a linear set of steps, creating a multidimensional grid of allowable design inputs. For a subset of analyses, the total couple length was also allowed to float. The unicouple results for each were scaled to the system level. The resulting solution space is parsed to find the optimal specific power configuration and response quantities for each GPHS and CPHS configuration.

The procedure above can be straightforwardly adapted to model the specific power of any RTG heat source which fits within the confinements of the assumed generator size. Substituting the mass of 1.61 kg per one 250 W GPHS heat source in place of one CPHS heat source allows for the direct comparison of specific powers between the CPHS and GPHS heat sources under multiple scenarios.

C. Fin-root Temperature Computation

1) Overview, Geometry, and Materials: The calculation of $T_{j,c}$ requires a calculation of the fin-root temperature (T_{fr}), where within the scope of this analysis, a temperature differential between T_{jc} and T_{fr} is assumed as 20 K and 30 K for a GPHS and CPHS RTGs respectively. For this calculation, a finite element conduction/radiation model was constructed utilizing the commercial software ANSYS Workbench (ANSYS INC, Canonsburg PA, USA). A computer aided design (CAD) model of a two-heat source RTG module was constructed within ANSYS Workbench Design Modeler. The CAD model consisted of an axial length of Aluminium-2219 housing equaled to $2N_{HS}$ times the axial length of each heat source. To the housing, 16 Aluminum-6062 radial fins were attached, assuming no thermal contact resistance. Housing and fin dimensions can be referenced in Tab. II. The thermal conductivities of the housing and fins were taken as 120 and 209 W/mK respectively. An emissivity $\epsilon = 0.93$ representing spacecraft thermal white paint was assumed for all radiating material.

2) Boundary Conditions and Governing Equations: The steady-state boundary-value problem assumed the thermal energy from the heat sources is uniformly distributed over the inner housing with an heat loss factor $Q_{loss} = 0.1$, leaving 90% of the total RTG heat exiting the generator in this manner. The cross-sectional areas perpendicular to the center RTG axis were assumed adiabatic as modularity had been assumed. The outer housing surface in addition to the fins were assumed to radiate to both each-other and open space. A cold-space vacuum temperature $T_{\infty,c} = 4$ K was assumed in all cases.

TABLE I
RTG TRADE-STUDY PARAMETERS

Nomenclature	*Parameter*	**Theroelectric Material**			
		SiGe		**MOD2**	
		GPHS	***CPHS***	***GPHS***	***CPHS***
N_{HS}	Number of heat sources	1:4:21	1:1:6	1:4:21	1:1:6
L [cm]	Converter leg length	1.6:0.1:2.0	1.3:0.1:1.7	0.8:0.1:1.2	0.7:0.1:1.1
L_s [cm]	Converter leg segment length	0.1:0.024:0.7	0.2:0.024:0.8	0.1:0.024:0.7	0.2:0.024:0.8
L_f [cm]	Fin length	7-28	10-28	7-28	10-28
t_{fr} [cm]	Fin root thickness	$L_f/64$	$L_f/64$	$L_f/64$	$L_f/64$
t_{ft} [cm]	Fin tip thickness	$t_f/4$	$t_f/4$	$t_f/4$	$t_f/4$
A_N [cm^2]	N-Leg area	0.01:0.02:0.30	0.02:0.02:0.50	0.01:0.02:0.30	0.01:0.02:0.30
A_P [cm^2]	P-Leg area	0.01:0.02:0.30	0.02:0.02:0.50	0.01:0.02:0.30	0.01:0.02:0.30
T_{jc} [K]	Cold-junction temperature	440:10:560	440:10:560	530:10:630	530:10:630

TABLE II
RTG DESIGN-CONSTRAINT PARAMETERS

Nomenclature	*Parameter*	*Value*
N_S	Number of parallel strings	4
Q_{loss} [%]	Heat loss factor	0.1
$D_{housing}$ [cm]	RTG Housing diameter	22.24
$t_{housing}$ [cm]	RTG Housing thickness	0.25
T_{jh} [K]	Hot-junction temperature	1273
$T_{\infty c}$ [K]	Cold space temperature	4
V_{design} [V]	Design voltage	30

The steady-state equation equation of conduction with constant thermal conductivity is given as

$$k\nabla^2 T = 0 \tag{1}$$

where the radiating heat flux on surface i to surface j is given by

$$\frac{Q_i}{A_i}\left(\frac{\delta_{ij}}{\epsilon_i} - F_{ij}\frac{1-\epsilon_i}{\epsilon_i}\right) = (\delta_{ji} - F_{ij})\sigma T^4. \tag{2}$$

Within Eq. (2), k is the aluminum's thermal conductivity, T denotes temperature, Q_i is the thermal energy leaving surface i, A_i is the area of surface i, δ_{ij} is the Kronecker delta, ϵ is the emissivity of the aluminum , and σ is the Stefan-Boltzmann constant. Finally, F_{ij} is the view factor of surface i on surface j, given by

$$F_{ij} = \frac{1}{A_i}\int_{A_i}\int_{Aj}\frac{\cos(\theta_i)\cos(\theta_j)}{\pi r^2}\,dA_j\,dA_i. \tag{3}$$

3) Solution Procedure: The CAD model was discretized into 3-dimensional 27-node quadratic finite elements. The weak solution to Eq. (1) was then obtained via the Galerkin Finite Element Method. To evaluate the radiation emitted from the body to itself and to cold space, Eqs. (2) and (3) were solved with Eq. (1) via a radiosity method of hemi-cubes [10].

D. Thermoelectric Power Computation

The thermoelectric power computation was determined on a unicouple basis, and then scaled to the system-level. For a given combination of seven trial parameters (n- and p-type areas and low temperature segment heights, cold junction temperature, total couple length, and load resistance), the system response quantities (SRQs) were determined using a mixed-methods analytic model. A one-dimensional thermal resistance network was constructed to model the hot- and cold-side geometries. Within this network, a fully-coupled thermal-electric unicouple model was integrated to solve the non-linear thermoelectric phenomena considering temperature-dependent material properties [11]. This iterative model was implemented in MATLAB (The Math Works Inc., Natick MA, USA). This model has been rigorously validated against high-resolution FVM models implemented in ANSYS CFX (ANSYS Inc. Canonsburg PA, USA) [12].

A number of constraints were applied to ensure the trial solution is physically valid. Any unicouple result with interfacial temperatures in excess of the maximum allowable temperature for a given material was omitted. If the solution contained only allowable temperatures, the number of couples was calculated to meet the desired voltage requirement via Eq. (4)

$$N_{couples} = N_{strings}\left(\frac{V_{design}}{V_{couple}}\right). \tag{4}$$

The required thermal inventory, which is defined as the heat input per unicouple times the number of couples, should not exceed the available thermal inventory, which is ideal thermal inventory times the quantity unity minus the heat loss factor. If the requirement was not met, the result was removed from consideration. Using this method, it was determined that any valid solution at maximum power would have an output voltage at the design voltage of the system. Lastly, an area constraint was applied to ensure that the necessary number of couples will fit within the RTG housing given a packing density.

To evaluate large design spaces, a number of methods were employed, including distributed multi-core computing, solver-initialization, heuristics for skipping expected invalid configurations, and Golden Section Search for maximizing power by modulating load resistance [13]. As an additional check, the model was further validated to existing configurations and SRQs for the SiGe GPHS-RTG [14].

E. Mass Model

Per each module, the masses of the housing and fins of each geometry were trivially computed taking the density of both

alloys as 2770 kg/m^3 from each CAD drawing in ANSYS Workbench. The masses of the thermoelectric converters were computed for each solution to the parametric design matrix from the resulting converter geometry, assuming an average density of 7000 kg/m^3. The GPHS and CPHS masses were taken as 1.61 and 5.36 kg respectively. The remainder of the generator material was approximated as a mass per unit length figure, derived from [7] by subtracting the housing, fin, converters, heat source, and end cap masses from the total mass of Next-Gen RTG concepts. This amounted to a 12.2 kg/m^3 load, where when multiplied by the distance, i.e, the axial height of the generator, a mass is obtained. The generator end cap mass was taken as 3.6 kg and added to the final total independent of the number of heat sources.

III. Results

The CPHS heat source was consistently found to produce a higher optimal specific power over the GPHS heat source for the allowable range of RTG thermal inventories. Optimal specific power is the largest W_e power per unit mass achieved by modulating design parameters. This increase in specific power is due to the higher CPHS energy density per unit mass over the GPHS, as shown Fig. 2. Additionally, Next-Generation converter materials (MOD2) are consistently seen to out-perform legacy SiGe materials as shown in Fig. 2. There is a marked increment in optimal specific power values with increasing thermal inventory, exhibiting an asymptotically increasing trend. This is due to the end-cap mass. With more heat sources, the end-cap's mass has less of a negative impact on the total system weight. That is, for low heat source designs, the end-cap masses contribute significantly to the total mass of the system, and do not contribute to the ability of the RTG to reject heat.

It is noted that taking a 4500 W_t limit due to shipping container design constraints, the maximum achievable specific power for the MOD2 and SiGe CPHS designs are 10.9 and 7.2 W_e/kg, respectively. In comparison, the MOD2 and SiGe GPHS designs achieve values of 9.2 and 6.3 W_e/kg, respectively, exceeding the goal of 8 W_e/kg [15]. It is evident the CPHS has the ability to provide higher optimal specific powers, while the use of newer thermoelectric materials provides greater performance increases in both the GPHS and CPHS.

The electrical power produced at the optimal specific power for the CPHS and GPHS-based RTGs is shown in Fig. 3, and the corresponding cold-junction temperatures are given in Fig. 4. In Fig. 3, it is seen achieving a higher specific power with a CPHS-based RTG requires a trade-off in power generated in regards to a GPHS-based RTG having identical thermal inventory. The GPHS-based RTGs, although attaining lesser specific powers for the use of SiGe and MOD2 converters, produce substantially higher electric power predictions than the CPHS counterparts. The measured electrical power output for the heritage SiGe-based GPHS-RTG as provided by Bennett et al. [14] is plotted in Fig. 3 as a reference for comparison.

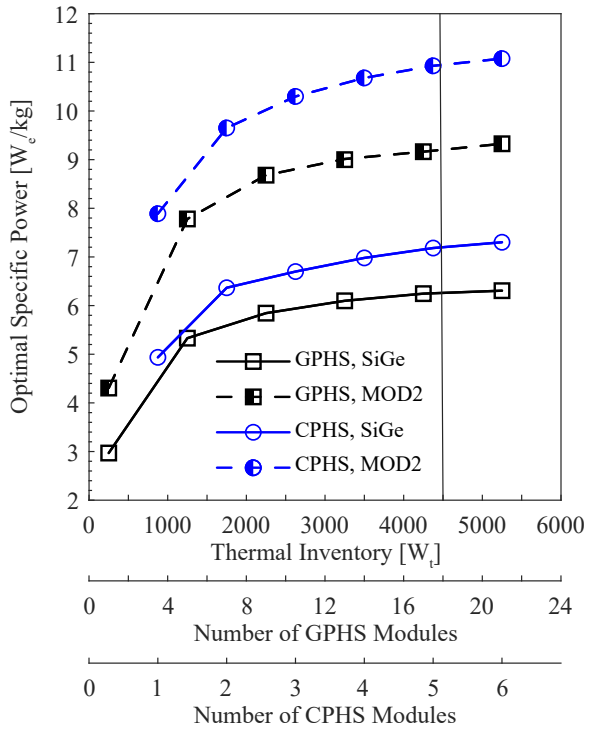

Fig. 2. CPHS versus GPHS-based RTG optimal specific powers as a function of thermal inventory and number of respective heat sources. The vertical line at 4500 W_t indicates US DOE 9904 shipping container design limit.

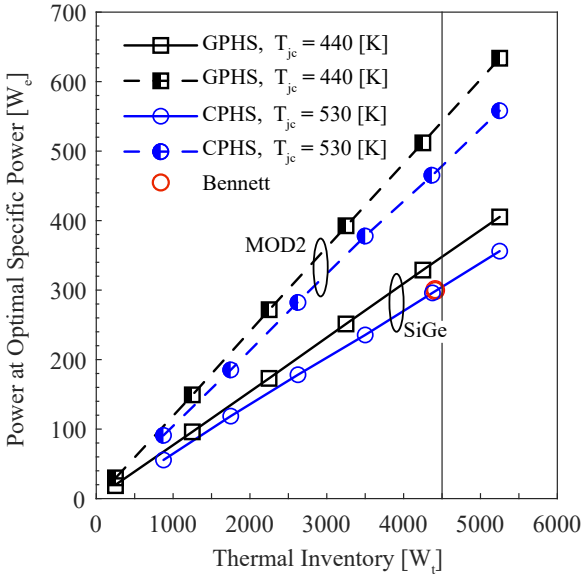

Fig. 3. The overall power produced by the GPHS-basd RTG is greater than that of CPHS-based RTG, highlighting a trade-off between maximizing specific power versus maximizing power. The GPHS RTG power output from the Bennett study [14] is reported for comparison. The vertical line at 4500 W_{th} indicates US DOE 9904 shipping container design limit.

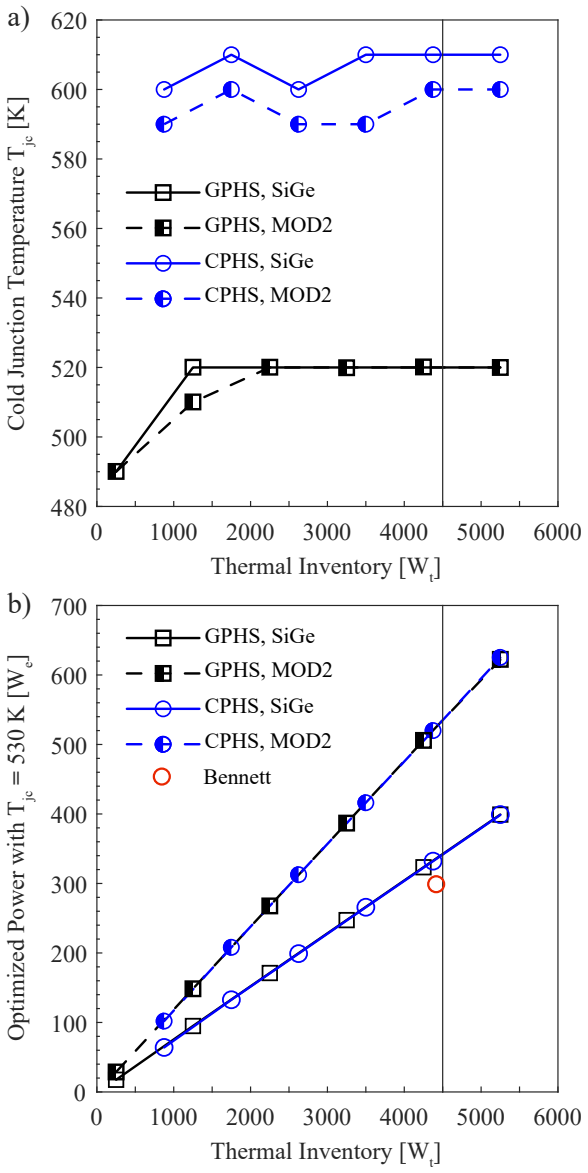

Fig. 4. a) The CPHS-based RTG attains its maximum specific consistently at higher temperatures than the GPHS-based RTG; these temperatures using both heat sources are all in excess of their maximum power condition T_{jc}. b) A comparison of power outputs at equal T_{jc} indicates the CPHS and GPHS-based RTGs would produce similar powers. The vertical line at 4500 W_t indicates US DOE 9904 shipping container design limit.

As shown in Fig. 4 a), the cold junction temperature at the optimal specific power for the CPHS is higher than that of the GPHS over the range of thermal inventories, due to higher energy density. For the CPHS to have comparable cold junction temperatures, and thus comparable power output at optimal specific powers (as shown in Fig. 4 b)), the fin sizes would have to increase. In doing such, the CPHS-based RTG could no longer fit within the US DOE 9904 shipping container, and there would also be a penalty in regards to optimal specific power.

In Figs. 5 and 6, the a) panels depict the power at optimal specific power for the SiGe and MOD2 converters, respectively, and all subsequent panels within each figure (b), c), etc.) depict converter geometry solutions for these aforementioned materials and heat sources. The converter lengths at optimal specific power are given in Fig. 5 b) for the SiGe converters and Fig. 6 b) for the MOD2 converters. Importantly, a CPHS-based RTG allows for a converter material length reduction by a factor of 1.85 for SiGe and MOD2 materials, in comparison to a GPHS-based RTG, considering shipping container thermal limits.

The specific power-optimal n-type converter areas are given in Fig. 5 c) and Fig. 6 c) for SiGe and MOD2 materials; the respective p-type converter areas are given in Fig. 5 d) and Fig. 6 d). The whiskers associated with the data points indicate the range of the bin for which results fell into, as listed in Tab. I. With increasing thermal inventory, the optimal converter configurations tend to have an increase in both n- and p-type areas with increasing thermal inventory to meet the design voltage constraint for four parallel converter strings.

The numbers of converter couples required to produce 30 V per each of four parallel converters is then calculated as per Eq. (4). The total number of required unicouples (i.e. considering four parallel converter strings) is shown in Fig. 5 e) and Fig. 6 e) for the SiGe and MOD2 materials, respectively. There is a non-linear trend with number of couples for increasing thermal inventory and the required voltage output, for the number of required couples is not a constraint for which other geometrical parameters are designed around as is done in conventional converter analyses.

Figure 7 depicts the maximum attainable power outputs per a given thermal inventory. In the current study, the maximum power outputs are limited by the radiator fin size required to dissipate the thermal energy such that the RTG would fit within the usable space of the US DOE 9904 shipping container. The higher thermal density offered by the CPHS requires a larger radiator; thus limiting the CPHS-based RTG power output over the GPHS-based RTG. The power output of the GPHS-RTG as provided by Bennett et al. [14] is shown for comparison. For a truly consistent power comparison at identical temperature differentials, Fig. 4 b) displays the power outputs of both CPHS and GPHS-based RTGs. Here, it is seen that, given identical T_{jc} and T_{jh} values, the power outputs are nearly identical between heat sources. The maximum power penalty encountered from operating at the optimal specific power state versus the maximal power state is 11% for a CPHS-based RTG versus and 10% for a GPHS-based RTG, and is shown in more detail in Fig. 8.

IV. Discussion

A. Compact heat source: from cryobots to general-purpose

Exploring the sub-surface oceans of icy worlds will likely require a more compact RPS than what is currently available. A CPHS is based on the repackaging of current technology, and is sufficient for providing the necessary thermal power density for such a mission. It has been extensively evaluated for its role in providing thermoelectric power at a system

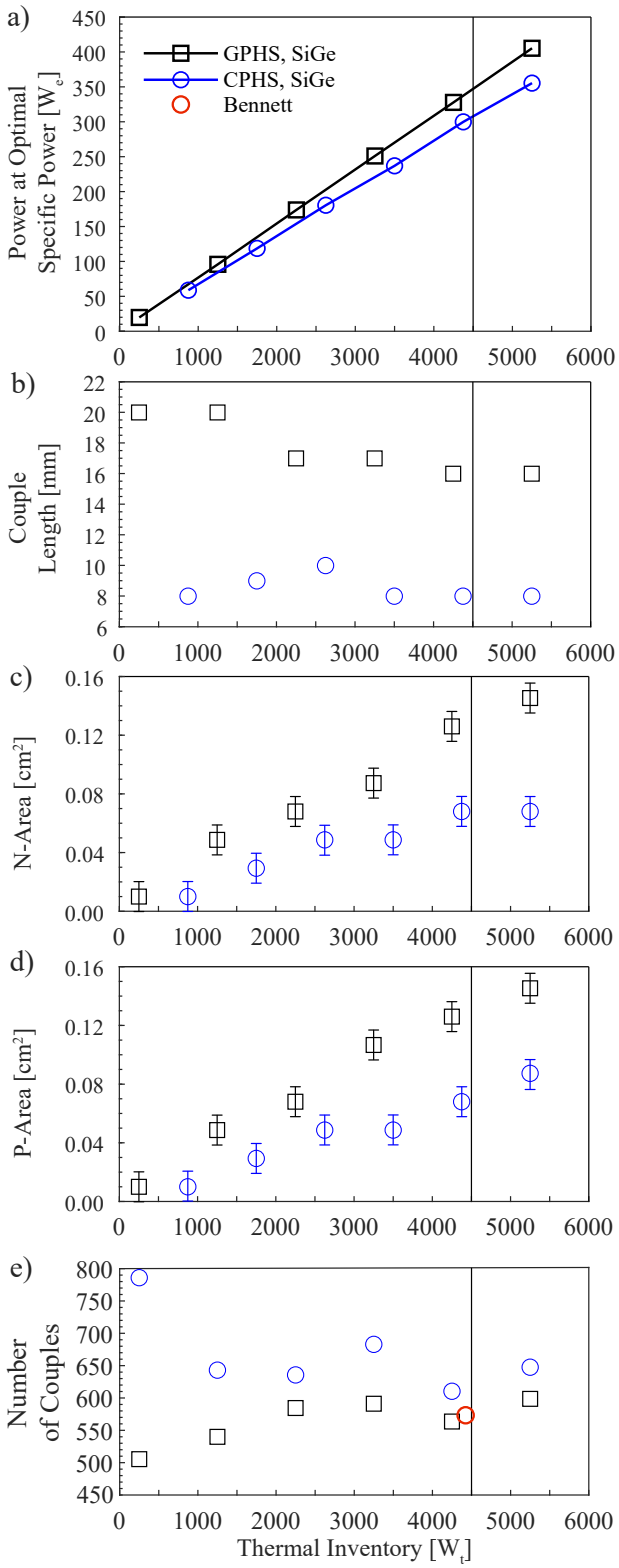

Fig. 5. SiGe converter a) Power at optimum specific power, b) couple lengths required to produce optimal specific power, c) area of n-type elements, d) area of p-type elements, and e) number of couples producing 30 V in each of four parallel strings at the optimal specific power. The vertical line at 4500 W_t indicates US DOE 9904 shipping container design limit.

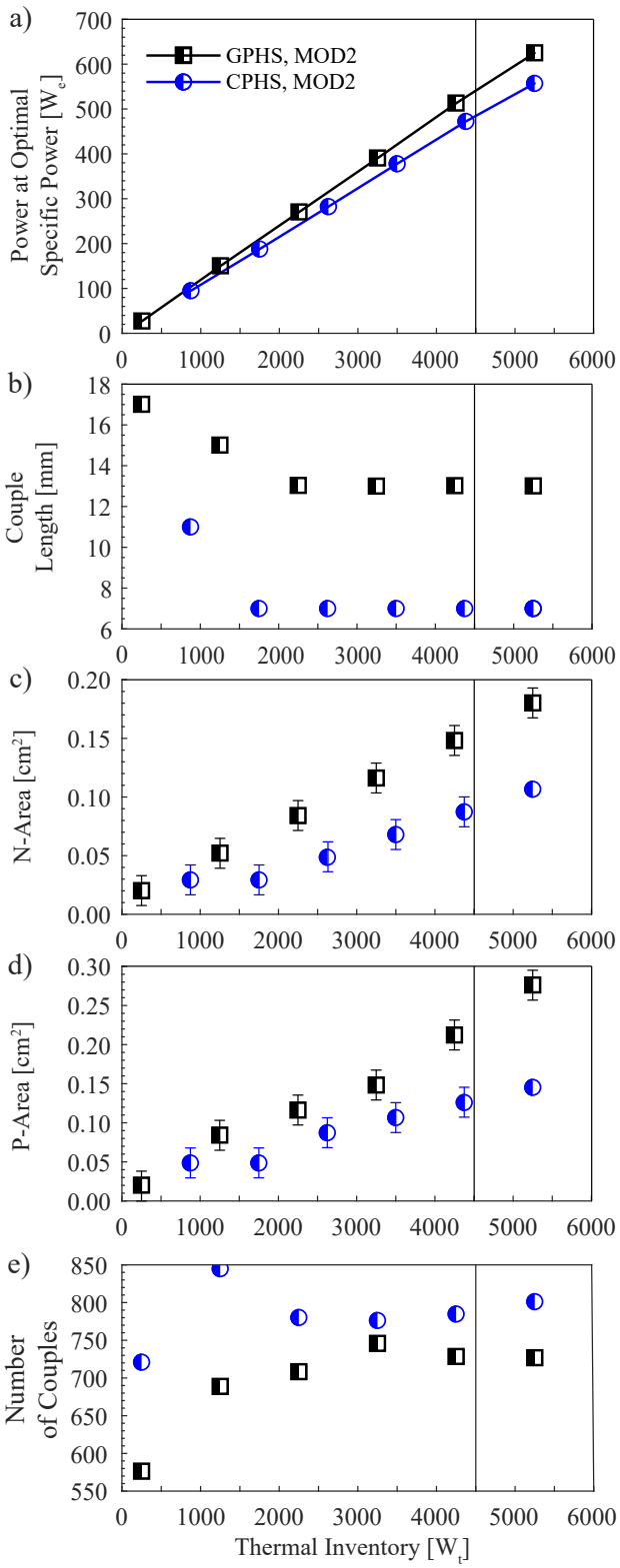

Fig. 6. MOD2 converter a) Power at optimum specific power, b) couple lengths required to produce optimal specific power, c) area of n-type elements, d) area of p-type elements, and e) number of couples producing 30 V in each of four parallel strings at the optimal specific power. The vertical line at 4500 W_t indicates US DOE 9904 shipping container limit.

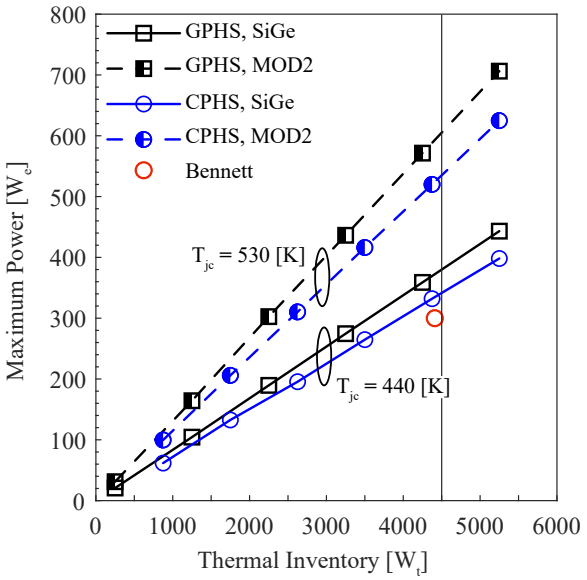

Fig. 7. The maximum attainable powers per a given thermal, limited by the radiator size compliant with the DOE 9904 shipping container dimensions. The power output of the GPHS-RTG in the Bennett study is shown for comparison. The vertical line at 4500 W_t indicates US DOE 9904 shipping container limit.

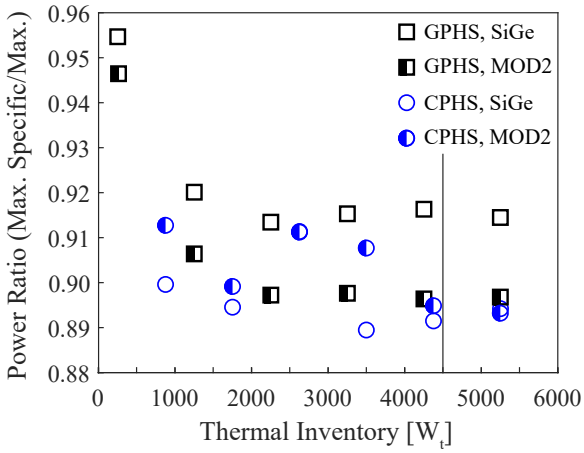

Fig. 8. The ratio of power at optimal specific power over power at optimal power (power ratio) for every case evaluated. There is no more than an 11% penalty taken in power output for maximizing specific power. Note the SiGe and MOD2 CPHS converters have the same ratio of power at approximately 2500 W_t.

level. To the authors' knowledge, the current study is the first of such analyses. An important finding from this study demonstrates that the CPHS can power RTGs to similar power output levels as the GPHS, and can additionally offer superior specific power performance over the range of thermal inventories examined. The CPHS-based RTG necessitates larger fin masses and higher cold junction temperatures to both radiate and conduct heat in comparison to the GPHS-based RTG. This is due to its higher energy density. While this is the case, the more compact arrangement of the CPHS-based RTG results in a significantly lower mass compared to the GPHS-based RTG at the same thermal inventory, with only marginally lower power output. This results in the CPHS-based RTG outperforming the GPHS-based RTG with respect to specific power.

Therefore, although initially designed specifically to act as a compact heater for cryobot missions, the current study suggests that the CPHS can also function as an alternative general purpose heat source for RTGs for several classes of missions. CPHS-based RTGs provide superior specific power in comparison to GPHS-based RTGs for both SiGe or Next-Gen $La_{3-x}Te_4$ 14-1-11 Zintl (i.e. MOD2) materials without sacrificing power output for a fixed hot and cold junction temperature differential. Further evaluation of a CPHS-based RTG at multiple levels may yield additional encouraging insights into the mission-enhancing and mission-enabling benefits of the device versus the challenges associated with its development.

The CPHS-based RTG models were shown to predict power output levels comparable to the GPHS-RTG with both SiGe or Next-Gen $La_{3-x}Te_4$ and 14-1-11 Zintl materials, with a clear performance improvement with the Next-Gen materials which deliver specific power levels exceeding 10 W_e/kg. Combining Next-Gen materials with the CPHS in an RTG could produce a viable power source for radioelectric propulsion missions which demand high specific power by simply repackaging TRL9-based technology. An example is the Centaur Orbiter New Frontiers Mission concept [8], where six Advanced Stirling Radioisiotpe Generators (ASRGs) are to deliver 150 W_e to an array of xenon Hall thrusters. The combination of Next-Gen $La_{3-x}Te_4$ thermoelectric converters and the CPHS would offer a solution for such missions utilizing technology involving the completion of existing technological developments and the repackaging of existing heat source technology.

B. Further development in cryobot technology concepts

The current study has shown the utility of the CPHS to encompass well beyond the realm of enabling cryobot missions to icy worlds. This is an important finding in respect to cryobot development because the cryobot-enabling CPHS can serve other purposes, while there is as of yet no planned icy world ocean access mission. The latest iteration of the NASA PRIME study evaluating mission concepts for Europan ocean access proposed a 10.5 kW_t CPHS-based thermal inventory would be necessary to successfully complete a sub-surface ocean access mission on Europa [2]. The notional estimate of ^{238}Pu production implies a roughly 17 year production period for the PRIME architecture thermal inventory assuming no further NASA-directed RPS missions are fueled over this time.

Furthermore, the United States Department of Energy's 9904 shipping container's thermal limit on the shipment of fissionable materials is limited to 4500 W_{th}. As such, there are ongoing efforts led by NASA's Jet Propulsion Laboratory to examine alternative modes of cryobot descent with the objective of reducing the required cryobot thermal inventory to below 4500 W_{th}. However, these efforts at the time of

the current study's completion are still ongoing; focusing in reducing the thermal inventory requirement from constantly maintaining a water annulus. Regardless of the minimum total thermal inventory required by a sub-surface ocean world access mission, a more compact heat source over the existing GPHS can only enhance the mission performance. In addition to the higher energy density, the hexagonal CPHS geometry conforms to a circular cross-section (ideal for ice probes) more so than the square GPHS geometry which, as described in [2], presents the deficiency of the colloquialism "a square peg in a round hole."

C. Limitations of current study involving device voltage and converter areas

The current study is a high-level theoretical direct comparison of the performance of two heat sources (the CPHS being only notional) powering a RTG, and attempted to keep many parameters fixed to achieve such a comparison. One fixed requirement was the number of parallel strings and the device voltage, kept at four and 30 V, respectively. At smaller thermal inventories, the voltage requirement, in conjunction with four versus two parallel strings, begins to demand smaller couple areas. Future work must consider a reduction in couple redundancy as well as direct current conversion technology (DC-to-DC) to relax the demand for smaller couple areas, most likely at a small cost of device performance. In the current study, the computed couple areas are reflective of the theoretical optimal performance of the device. Trade studies particular to these lower inventory RTGs individual to a design must be conducted to increase the couple areas and/or design voltages such that the detracted power is minimal. Such a goal is beyond the deliverables of the current study.

D. Other limitations and future directions

The analysis presented is a high-level analysis designed to directly compare the thermoelectric performance of a novel compact heat source versus the already flown GPHS keeping fixed as many parameters as possible when making the comparison. As such, the details of much of the structural and heat-collecting hardware have been simplified or idealized in this comparison, and it is assumed that existing GPHS-based hardware such as the hot and cold shoes and thermal insulation will behave comparably. In this study, only seven parameters (n-type/p-type areas, n-type/p-type low temperature segment heights, cold junction temperature, total couple length, and load resistance) were considered, though exhaustively. In real generators, there are many more design parameters to consider (sizing of interconnectors, wiring, constraining unicouples mechanically, etc.). To account for these other design parameters, a much more expansive analysis will be required.

To refine the analysis at the converter level, there are a number of improvements that can be considered. The solver employed in this analysis is capable of accounting for the effect of electrical/thermal contact resistances and interconnectors on a unicouples's performance with small modifications [11]. Further, parasitic losses, such as radiative heat loss, occurring around the unicouple legs can be predicted by leveraging a radiation view factor lookup table generated by a GPU view factor solver [16]. This would be extensible to more rapidly evaluating possible fin design modifications.

Further, it would be worth explicitly coupling the fin's thermal profile into the thermal resistance network for the unicouple, such that some assumptions at the system-level can be removed. This, in combination with considering view factor variance along the length of the generator, would lead to a more intricate and methodical analysis.

Outside the generator, with respect to operating conditions, it is furthermore assumed the view factor with increasing or decreasing generator length remains approximately the same. All cold junction temperatures were based on operation in cold space, and operation in more radiation-intense or non-vacuum environments were beyond the scope of the current analysis. All power calculations assume beginning of life levels and device degradation is beyond the scope of this analysis. This analysis does however suggest that much can be gained from more intricate studies which incorporate more fidelity as well as mission environments in terms of enhancing future RPS missions.

Additionally, future analysis at some point must also include a study on the criticality of the CPHS. This is due an increase in an average thermal density by a factor of 1.97 in a CPHS stack versus a single stack of GPHS [2]. Thus, a higher density of alpha-decay from the ^{238}PuPu isotopes is to be expected than previously considered in studies such as [9]. In this study, it was determined that nearing criticality would require more than 1000 Step-2 GPHS blocks stacked in a cubic-based arrangement. This would amount to roughly 250kW of thermal inventory - roughly a factor of 20 times that of the proposed cryobot thermal inventory herein. Although the geometry and packaging of the CPHS is different from the GPHS requiring a similar analysis to be repeated, the large margin by the current estimate is encouraging. Further steps in this direction would include analysis on the impact of mission radiation environments on the CPHS, as well as the consequences of human exposure to CPHS-based radiation.

V. Conclusions

Currently, only the general purpose heat source, or GPHS, is available to radioisotope power systems to support many proposed ambitious missions for which solar, chemical or stored power systems are not viable. The compact heat source, or CPHS, has been proposed for enabling cryobot ocean-access missions on the moons of the outer planets. Utilizing novel fast-compute codes in parametric studies, the current study was able to consider a multitude of RTG design parameters to deeply explore and compare the performances of the two heat sources using heritage (SiGe) and Next-Generation (MOD2) converter materials.

The current analysis has demonstrated at a high level that the CPHS is integrable with existing and Next-Generation thermoelectric converter technology. Additionally, due to the use of less thermoelectric material to produce electrical power

per an equivalent GPHS-based thermal inventory, a CPHS-based RTG can produce a higher specific power than a GPHS-based RTG per a given thermal inventory. The CPHS with legacy SiGe and MOD2 materials can achieve specific powers of 7.2 and 10.9 W_e/kg, far above the ability of the GPHS to deliver specific powers of 9.2 and 6.3 W_e/kg using the same novel and legacy materials, respectively. This notion suggests the CPHS can be mission enabling as well as mission enhancing for classes of missions other than cryobot missions while requiring minimal technological development. Further analysis at both higher and lower levels is recommended to explore the means by which future RPS-based missions could leverage the CPHS enable or enhance future missions.

ACKNOWLEDGMENT

The authors would like to give their profound gratitude to the University of Pittsburgh's Center for Research Computing. This research was carried out at the Jet Propulsion Laboratory, California Institute of Technology, under a contract with the National Aeronautics and Space Administration and at the University of Pittsburgh. The information in this paper about future RPS is predecisional and is provided for planning and discussion purposes only.

REFERENCES

[1] J. Moore, L. Spilker, M. Cable, S. Edgington, A. Hendrix, M. Hofstadter, T. Hurford, K. Mandt, A. McEwen, C. Paty, and L. Quick, "Exploration strategy for the outer planets 2023-2032: goals and priorities," arXiv preprint arXiv:2003.11182.

[2] D. Woerner, S. Johnson, J.-P. Fleurial, S. Howell, B. Bairstow, M. and Smith, "Radioisotope heat sources and power systems enabling ocean worlds subsurface and ocean access missions," *Bulletin of the American Astronomical Society*, vol. 53, no. 4, p. 322, May 2021.

[3] S. Howell, "The likely thickness of europa's icy shell," The *Planetary Science Journal*, vol. 2, no. 4, pp. 129, August 2021.

[4] B. Cassler, M. Smith, M. Durka, B. Furst, B. Hockman and M. Ullman, "Constraints on the behavior of a descending ice probe due to force balance", *Acta Astronautica*, vol. 189, pp. 606–614, December 2021.

[5] H. Aamot, "Heat transfer and performance analysis of a thermal probe for glaciers," *US Army Materiel Command, Cold Regions Research & Engineering Laboratory*, vol. 194, 1967.

[6] P. Ferrell, "Radioisotope thermoelectric generator transportation system safety analysis report for packaging. Volumes 1 and 2," No. WHC-SD-RTG-SARP–001. Fluor Daniel Hanford, 1996.

[7] Nuclear Power Assessment Study Final Report, NASA Contract NNN06AA01C, February 2015.

[8] S. Oleson and M. McGuire, "COMPASS final report: radioisotope electric propulsion (REP) centaur orbiter new frontiers mission," Glenn Research Center, Cleveland Ohio, 2011.

[9] R. Lipinski and D. Hensen, "Criticality calculations for step-2 GPHS modules," *AIP Conference Proceedings*, vol. 969, no. 1, pp. 452–457, 2008.

[10] M. Cohen and D. Greenberg, "The hemi-cube: a radiosity solution for complex environments," *ACM Siggraph Computer Graphics*, vol. 19, no. 3, pp. 31–40, July 1985.

[11] S. Wielgosz, K. Yu, A. Mamoozadeh, F. Drymiotis, M. Durka, B. Nesmith, J.-P. Fleurial and M. Barry. "Mathematical and numerical modeling of next-generation segmented thermoelectric converters with electrical and thermal contact resistances," unpublished.

[12] S. Wielgosz, C. Clifford, K. Yu and M. Barry. "Fully-coupled Thermal-electric Modeling of Thermoelectric Generators," unpublished.

[13] S. Riley, S. Wielgosz, K. Yu, M. Durka, B. Nesmith, F. Drymiotis, J.-P. Fleurial and M. Barry, "Optimization Methods for Segmented Thermoelectric Generators," ASTFE Digital Library, Begel House Inc., 2022.

[14] G. Bennett et al., "Mission of daring: the general-purpose heat source radioisotope thermoelectric generator," *4th International Energy Conversion Engineering Conference and Exhibit (IECEC)*, pp. 4096, June 2006.

[15] "*NASA Technology Roadmaps, TA 3: Space Power and Energy Storage*," May, 2015. Accessed on: Oct. 14, 2022. Available: https://www.nasa.gov/sites/default/files/atoms/files/2015_nasa_technology_roadmaps_ta_3_space_power_energy_storage.pdf

[16] A. Hancock, L. Fulton, J. Ying, C. Clifford, S, Sammak and M. Barry, "A GPU-accelerated ray-tracing method for determining radiation view factors in multi-junction thermoelectric generators," *Energy*, vol. 228, pp 120438, 2021.

[17] W. Kelly , N. Low , A. Zillmer , G. Johnson ,and E. Normand "Radiation Environments and Exposure Considerations for the Multi-Mission Radioisotope Thermoelectric Generator," *AIP Conference Proceedings* 813, 906 (2006); https://doi.org/10.1063/1.2169273